4th Specialty Conference on Coastal, Estuary and Offshore Engineering
4e Conférence spécialisée sur l'ingénierie côtière et en milieu maritime

Montréal, Québec
May 29 to June 1, 2013 / *29 mai au 1 juin 2013*

Modeling of the Attenuation of Hydraulic Bores by Coastal Forests using the SPH Method

S. Piché[1], I. Nistor[2]
[1]Graduate Student, Dept. of Civil Engineering, University of Ottawa, Canada
[2] Associate Professor, Dept. of Civil Engineering, University of Ottawa, Canada

Abstract: The attenuation of large hydraulic bores, such as the ones induced by the breaking of tsunamis, near the shoreline, can result in massive damage to infrastructure and significant loss of lives. Man-made structures such as seawalls and breakwaters are beneficial for restricting the inland propagation of waves, but may be costly and ineffective during large tsunami events. Natural structures, such as coastal forests, may provide a reasonable method for the protection of coastal regions, as they are capable of attenuating the bore flow and restricting the movement of debris. This paper will present the results of a numerical model based on the Smoothed Particle Hydrodynamics (SPH) method that was used to simulate the attenuation and propagation of a hydraulic bore on a coastal forest. The SPH method uses a Lagrangian approach which allows for an accurate reproduction of the bore propagation, breaking and splashing as well as alleviating problems that may occur for traditional computational methods. The open source-code software (DualSPHysics), which uses the Graphical Processing Unit for faster computational time, was used to run the simulations. The model was used to determine a relation between the number and density of the vegetation elements (such as trees) and their effect on the bore attenuation and velocity.

1 Introduction

Tsunamis are considered to belong to the class of long gravity waves and are usually generated by landslides or underwater seismic activity. Coastal protection against tsunamis includes both man-made and natural protection, such as seawalls or coastal forests. Though it has been found that coastal forests are not wholly effective in preventing flooding, they are capable of reducing impact forces and flow depths and velocities which limits the amount of damage caused by the flooding [Forbes and Broadhead 2007]. The coastal forest acts as a barrier which reflects a portion of the wave energy seaward and allows the rest to infiltrate the forest. As the wave propagates through the forest the wave energy is slowly dissipated by the friction caused by the trees. The total deduction in wave depth and velocity is dependent on how much water is reflected at the front of the forest and how much energy is absorbed [Forbes and Broadhead 2007].

A significant amount of research has been done dealing with the effectiveness of coastal forests and vegetation belts on the dissipation of tsunami bores striking coastal areas. The effectiveness of reduction of the tsunami impact and attenuation is dependent on various tsunami parameters such as the amplitude of the approaching tsunami wave, its period, the amount of waves in the tsunami and the wave length; as well as on coastal forests parameters such as the coastal geometry, the width and height of the coastal forest belts, the density of the forest and the individual characteristics of the trees themselves. This results in large variations in the forests effectiveness based on its specific coastal parameters.

Nandansena et al. (2008) examined the reduction in tsunami energy using an enhanced one-dimensional numerical model for different ground slopes and tsunami periods with different forest widths. Findings indicated larger reductions behind the forest for gentler slopes (2.8% for 1:50 slope and 37% for 1:1000 slope), while the wave period was found to have little effect. Gelfenbaum et al. (2007) examined the effect of mangrove stem density and found that increasing the mangrove density decreased the maximum water level and run-up, with a reduction of 9 to 20% in the water level. Yanagisawa et al. (2009) studied the fragility of the mangrove trees and used this to develop a model to estimate the tsunami reduction based on the damage probability of the trees. Additional studies in this field include examining the effect of the forest width [Ohira 2012, Harada et al. 2005], the density of the trees [Iimura et al. 2012, Hiraishi et al. 2003, Harada et al. 2005], the formation of the trees in the forest [Irtem et al. 2008] and the period of the tsunami wave [Harada et al. 2005]

The study presented in this paper focused on the reduction in tsunami run-up and inundation caused by varying forest densities, widths and tree formations using a 3-dimensional SPH numerical model.

2 The SPH Model

The Smoothed Particle Hydrodynamics (SPH) method is a mesh-free Langrangian method which was first introduced by Gingold and Monaghan (1977) and Lucy (1977) for the modeling of astrophysical and cosmological phenomena. In the early nineties Monaghan (1994) applied this method to the study of fluid dynamics. Applications for this method now include both computational solid mechanics as well as computational fluid mechanics. A more comprehensive analysis of the SPH formulation can be obtained from Liu and Liu (2003), Monaghan (2005) and St-Germain (2012).

The SPH method functions by representing the physical domain using a set of arbitrarily distributed particles which possess individual properties, such as mass, velocity and pressure. The approximation of these properties for an individual particle, i, can be calculated using the functional approximation:

[1] $$f(\mathbf{x}_i) = \sum_{j=1}^{N} \frac{m_j}{\rho_j} f(\mathbf{x}_i) W_{ij}$$

where $\mathbf{x}_i$ is the position vector of particle i, m_j and ρ_J are the mass and density of the neighboring particle j, respectively. W_{ij} represents the weighting function, also known as the smoothing kernel:

[2] $$W_{ij} = W(\mathbf{x}_i - \mathbf{x}_j, h)$$

where h is the smoothing length which controls the size of the influence domain for particle i. There are a variety of weighting function, this study used the cubic spline which is defined as:

[3] $$W_{ij} = \alpha_D \begin{cases} 1 - \frac{3}{2}q^2 + \frac{3}{4}q^3 & 0 \le q \le 1 \\ \frac{1}{4}(q)^3 & 1 \le q \le 2 \\ 0 & q \ge 2 \end{cases}$$

where $q = r_{ij}/h$ and $\alpha_D = 5/(\pi 4h^3)$ for three-dimensional space.

The governing equations used in the SPH method are derived based on the physical conservation laws. They are represented by the compressible Navier-Stokes equations for momentum and continuity. These are:

[4] $$\frac{Du_i}{Dt} = -\sum_{j=1}^{N} m_j \left(\frac{P_i+P_j}{\rho_i \rho_j}\right) \nabla_i W_{ij} + \mathbf{g} + \text{Diffusion Terms}$$

and

[5] $$\frac{D\rho_i}{Dt} = \sum_{j=1}^{N} \frac{m_j}{\rho_j} (\mathbf{u}_i - \mathbf{u}_j) \cdot \nabla_j W_{ij}$$

where $\mathbf{u}_i$, $\mathbf{u}_j$, P_i and P_j are the velocity vectors and pressures for particles i and j, respectively. The SPH formulation offers different diffusion terms to represent the viscosity effects. The term used in this study was laminar viscosity with a sub-particle scale turbulence (SPS):

[6]

where v is the kinematic viscosity of laminar flow and τ is the SPS stress tensor element.

Last, is the equation of state, modified by Monaghan (1994), which allows for the calculation of the pressure term in the momentum equation without the need to solve additional partial differential equations.

[7] $$P_i = \frac{c_0^2 \rho_0}{\gamma} \left[\left(\frac{\rho_i}{\rho_0}\right)^{\gamma} - 1\right]$$

where γ can be taken as 7, ρ_0 is the reference density and c_0 is the speed of sound in the water for the reference density. The pressure field of the particles simulated using the SPH can be subject to large pressure oscillations. This problem was overcome by the use of a Shepard density filter. The filter is applied every M time steps, with M on the order of 30. This filter is represented by:

[8] $$\rho_i = \frac{\sum_j \rho_j \overline{W}_{ij} V_j}{\sum_j \overline{W}_{ij} V_j}$$

where the kernel has been corrected using a zeroth-order correction

[9] $$\overline{W}_{ij} = \frac{W_{ij}}{\sum_j W_{ij} \frac{m_j}{\rho_j}}$$

3 Computational Domain

The study required the generation of solitary waves in a domain with a sloped bottom of 1:10; the prototype domain, Figure 1 had an initial water depth of 2.25 m. The walls and bottom of the computational domain were modeled using fixed boundaries, while the downstream end of the model contained a wave maker with imposed movement to generate the solitary wave. The initial computation domain shown in Figure 2 had a water depth 0.03 m below the prototype depth due to the particle spacing.

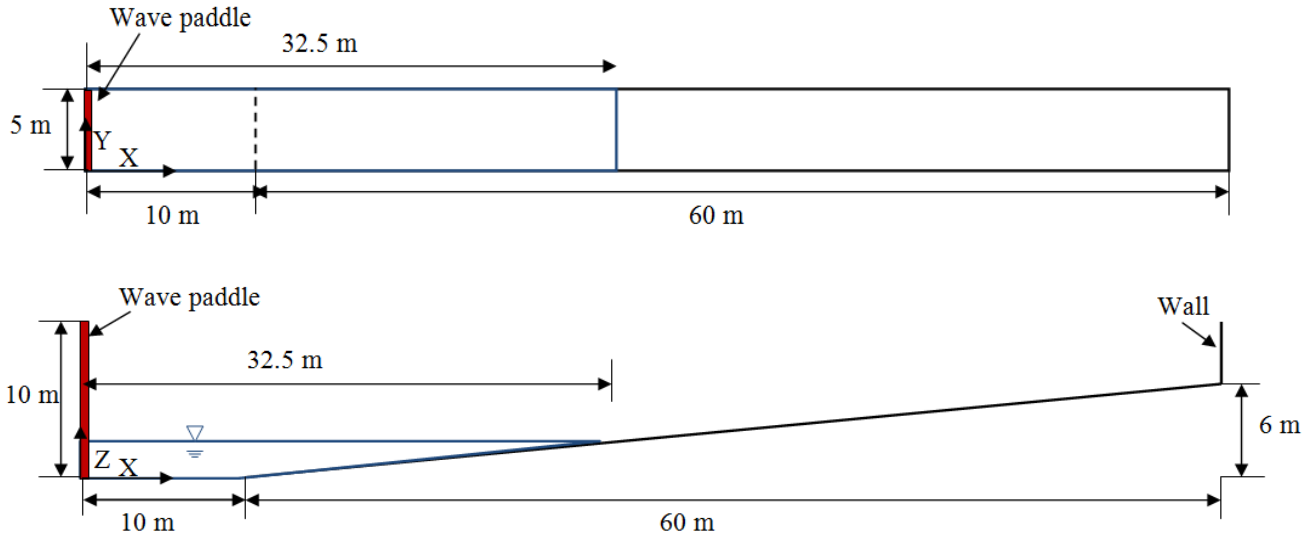

Figure 1: Plan and Side View of the Prototype Domain

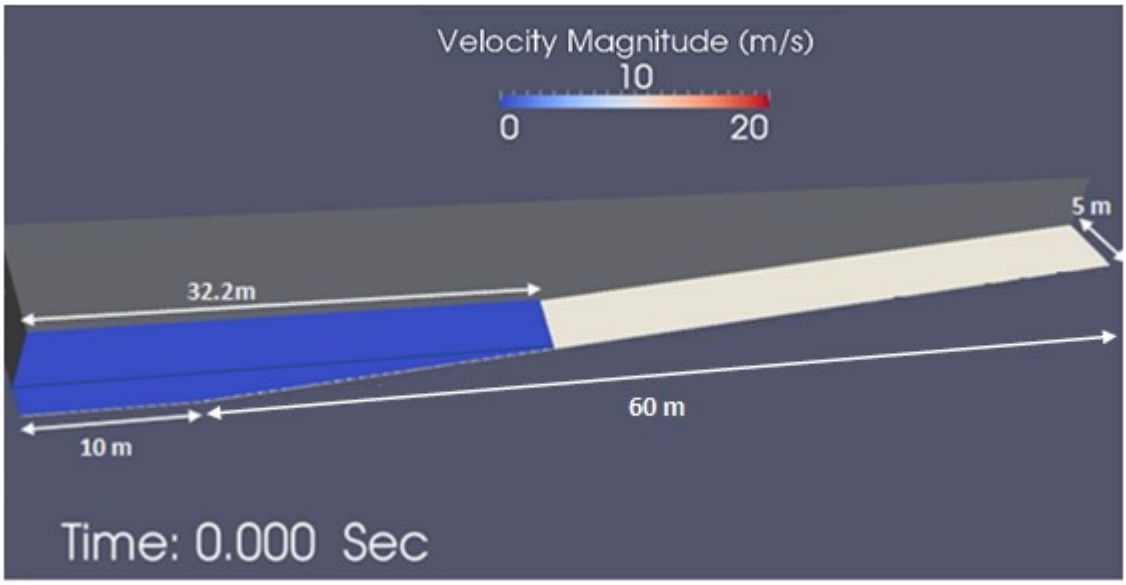

Figure 2: Computational Domain

The solitary wave used in this study was 2.5 m in height for the prototype water depth of 2.25 m. The movement of the downstream wave maker was calculated based on the amplitude of a theoretical solitary wave, Figure 3, with the movement and velocity of the wave maker being obtained from equations derived from Hughes (1993), shown in Figure 4.

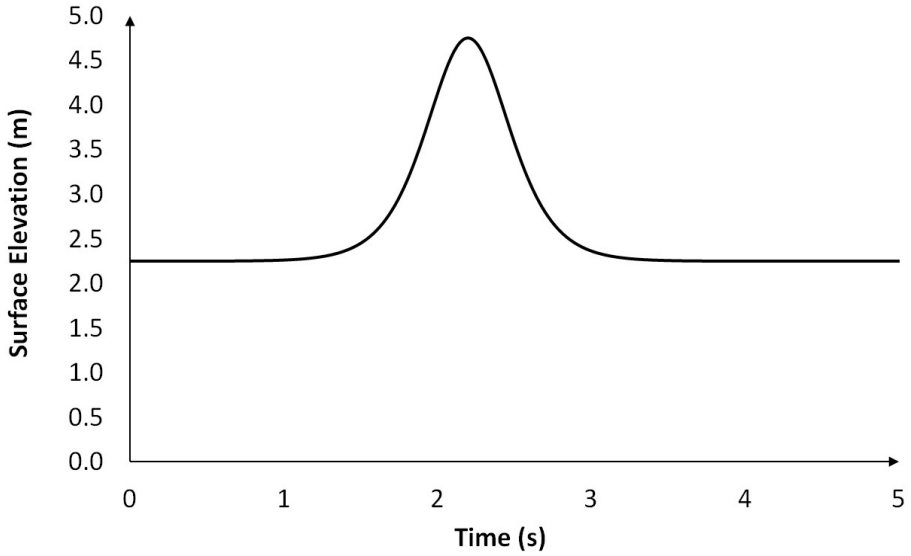

Figure 3: Theoretical Solitary Wave

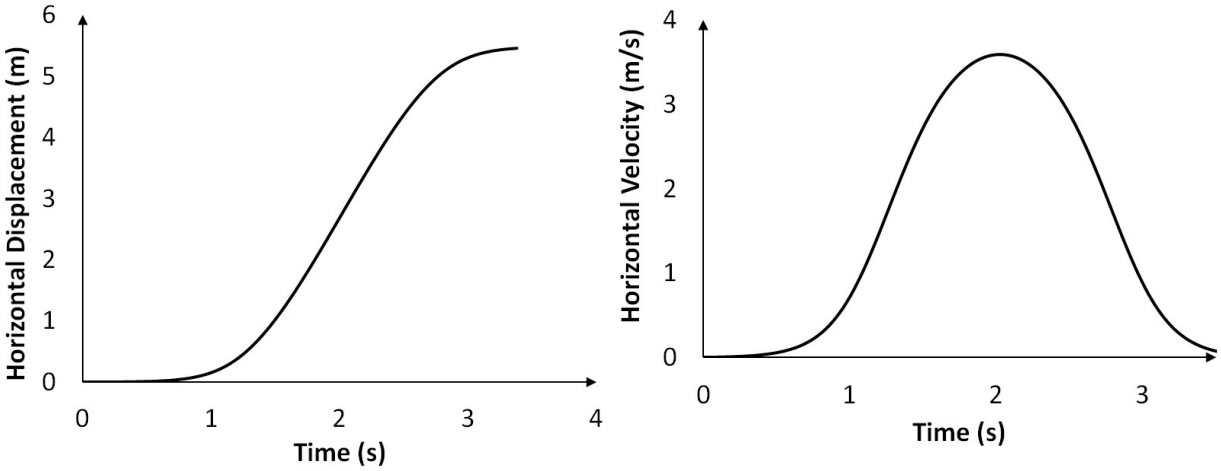

Figure 4: Relative Wave Board Motion (Left) and Relative Wave Board Velocity (Right)

The scenarios performed for this study are shown in Table 1.

Table 1: Study Scenarios

Formation	Number of Trees per Row	Number of Rows	Tree Diameter (m)	I_y (m)	I_x (m)
No Trees	0	0	N/A	N/A	N/A
Rectilinear	1-5	1-3	0.25	0.88 – 2.625	0.88 – 2.625
Staggered	2-4	2-3	0.25	0.583 - 1.05	1.166 - 2.1

The location of the simulated trees is dependent on the run; Figure 5 shows a sample of the rectilinear and staggered formations.

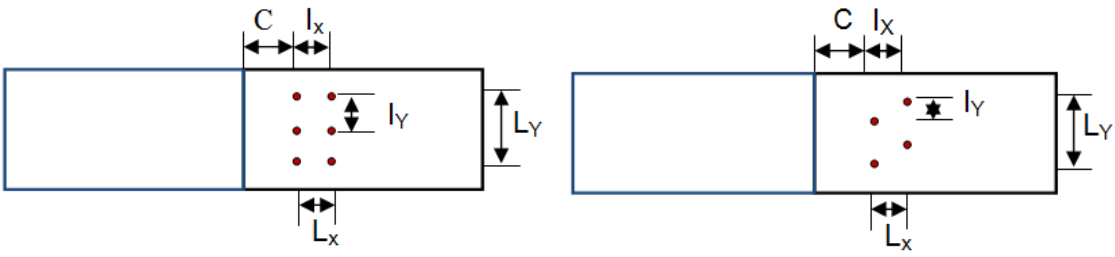

Figure 5: Dimensions of Tree Spacing for Rectilinear (Left) and Staggered (Right) Formation

The rectilinear formation contains trees in rectangular rows with identical spacing in the l_x and l_y directions. The L_x and L_y values are dependent on the number of trees and amount of rows used in the simulation. The staggered formation uses trees in offset rows, with the distance l_x being equal to the spacing between the trees in each row, which is twice the distance between the trees, l_y. In all cases, the distance, C, from the still-water level to the first row was the same.

The measurements obtained from the model include seven velocity measurements, locations shown in Figure 6, as well as the maximum attenuation of the solitary wave.

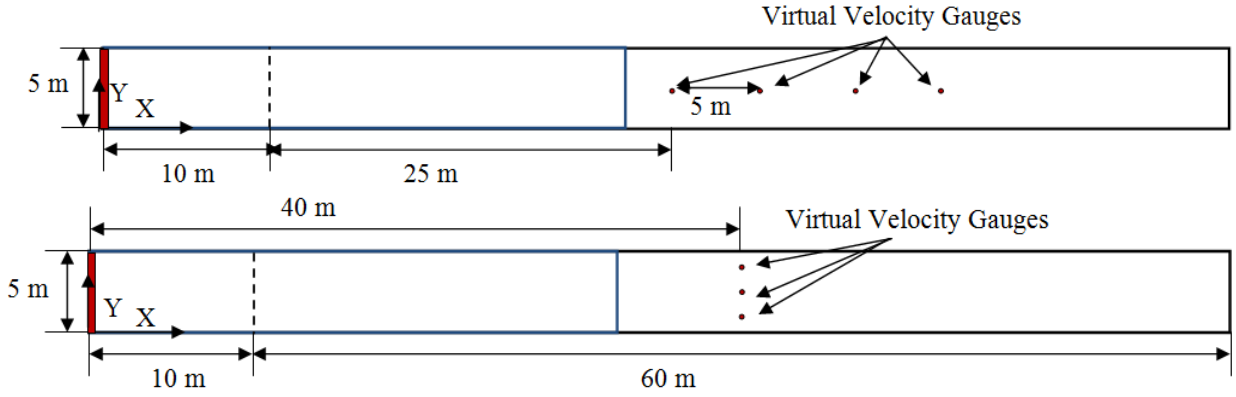

Figure 6: Virtual Velocity Gauge Locations

4 Discussion of Results

The results obtained from this study are shown in this section. The velocities for the formation with no trees are compared with those obtained for a single tree to give an indication of the reduction of velocities which can be expected. This section also examines the effect of the forest formation, rectilinear or staggered, and the amount of rows on the run-up and inundation of the solitary wave.

4.1 Wave Velocity

The variations found in the solitary wave velocity across the domain width and length gives a good indication of the coastal forests effect on the inland propagation. Figure 7 shows the reference formation, with no trees, which indicates that the broken wave propagates as a hydraulic bore with almost constant velocity across the width of the domain. Larger variations can be seen in the run-down of the wave. Figure 7 (b) shows that the largest wave velocity is obtained from 35-40 m which is located just inland of the still-water level. Positive velocities seen past 35 seconds is caused by the wave reflection as the wave returns to the horizontal section of the domains bottom.

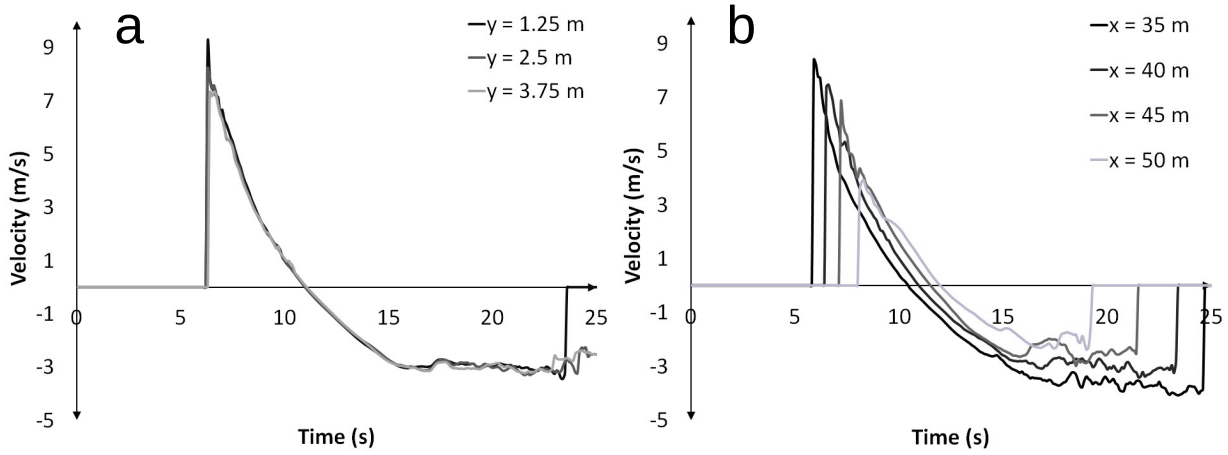

Figure 7: Velocity Measurements for No Trees a) Across the Domain Width at 40 m and b) Across the Domain Length through the Center

For the formation with one tree, shown in Figure 8, there is a visible reduction in the magnitude of the highest run-up velocity of approximately 1 m/s as. Additionally Figure 8 (b) indicates that there is a shorter duration of propagation, which can be seen across the length of the domain. The reflection seen in the initial scenario is also visible in this case as well.

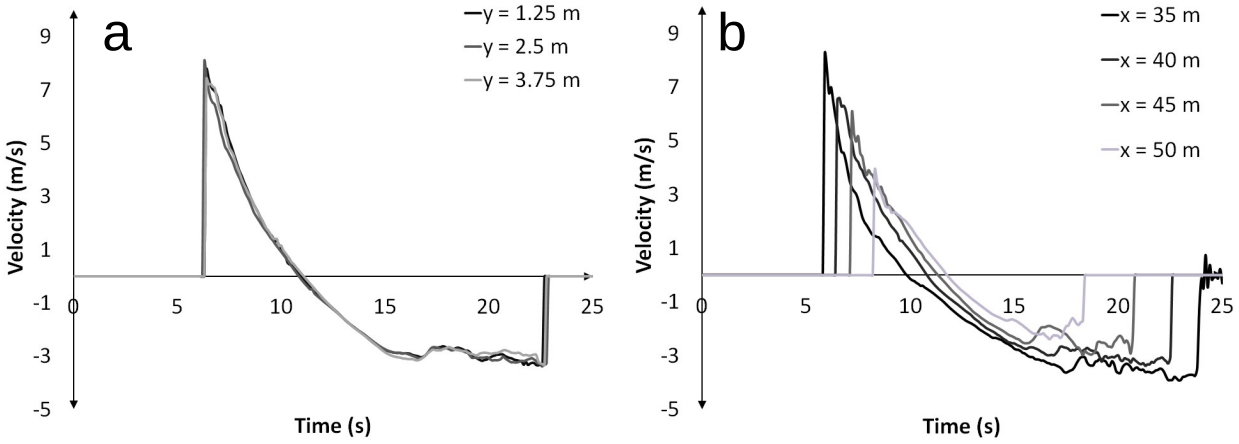

Figure 8: Velocity Measurements for Single Tree a) Across the Domain Width at 40 m and b) Across the Domain Length through the Center

4.2 Run-up Height and Inundation

Variations in the vertical run-up height and the inundation distance for the rectilinear and staggered formations can be seen in Figures 9 and 10. Both of these figures show a decrease in the overall run-up and inundation as the amount of trees per row increases, as the density increases, as well as for increasing amount of rows, an increase in the forest width. As the slope of the shoreline is constant for all of the simulations the vertical run-up and inundation show similar profiles.

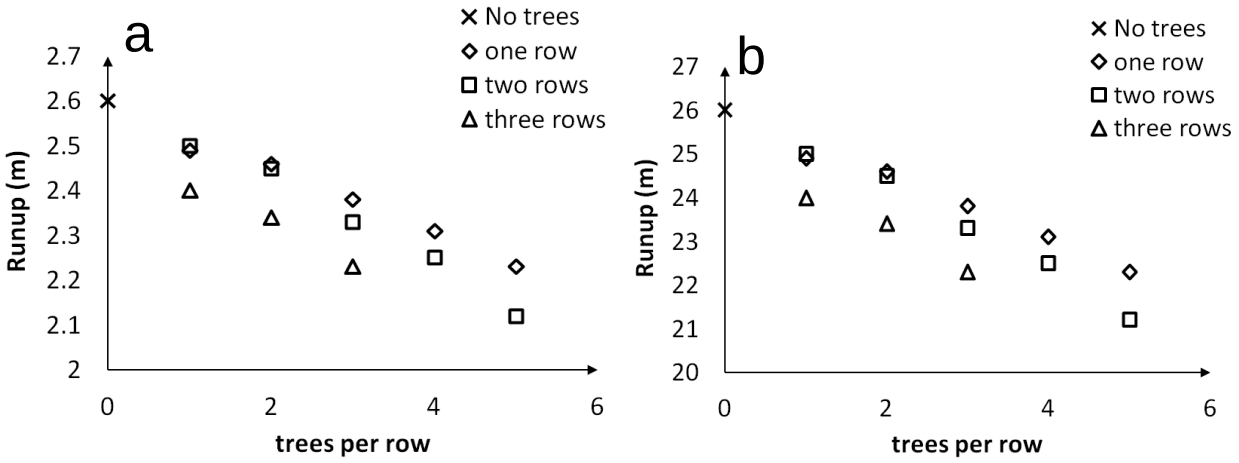

Figure 8: Run-up Measurements for a) Vertical Run-up and b) Inundation for Rectilinear Formation

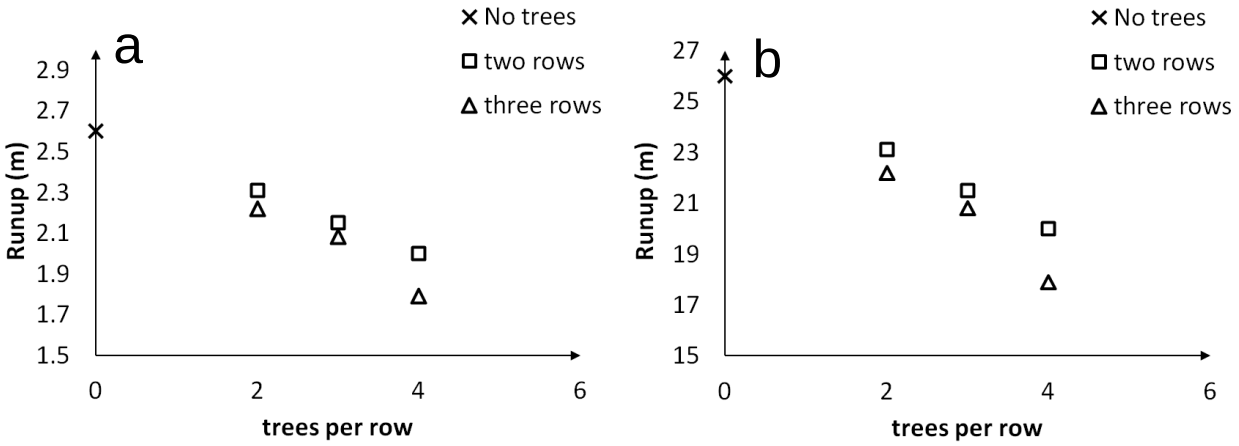

Figure 9: Run-up Measurements for a) Vertical Run-up and b) Inundation for Staggered Formation

Table 2 provides the results with respect to the reduction of run-up height. The results in this table indicate that the largest reduction in run-up and inundation is caused by the staggered formation. It is believed that this is caused by the formations ability to form a barrier with no straight flow path around the trees. It can also be seen from the results that an increase in the width of the forest and in the density of the trees will result in a reduction of the wave run-up.

Table 2: Reduction Rate (%) for Wave Run-up

Number of	Rectilinear			Staggered	
trees per row	1 Row	2 Rows	3 Rows	2 rows	3 rows
1	4.2	3.8	7.7	-	-
2	5.4	5.8	10.0	11.2	14.6
3	8.5	10.4	14.2	17.3	20.0
4	11.2	13.5	-	23.1	31.2
5	14.2	18.5	-	-	-

5 Conclusions and Future Work

This intent of this study was to examine the effect of coastal forests on the propagation of a tsunami solitary wave using a Langrangian numerical model. This model represented the trees as cylindrical piers, with a diameter of 0.25 m, which were placed above the still-water level along a shoreline with a slope of 1:10. This study examined the effect of two different coastal forest formations, staggered and rectilinear, using a varied amount of rows and trees per row for each simulation. The study results can be summarized as follows:

1) The staggered formation was more effective then the rectilinear formation at reducing the tsunami inundation and run-up. Results indicate that the rectilinear formation was able reduce the run-up and inundation by 4.2 to 18.5%, based on the amount of rows and the density of the trees. The staggered formation was able to reduce the inundation and runup by 11.2 to 31.2%.
2) Additional rows in the formation result in a decrease in the tsunami run-up and inundation. This reduction becomes more substantial as the width of the forest increases.

Future work in this field should include examining the effect of the water depth and tsunami wave height on the reduction of the inundation and run-up and examining the effect of the different factors on each other in order to get a complete understanding of the different coastal parameters. Additional research could also be performed in the analysis of the coastal forests effect on the run-down of the tsunami bore.

References

Forbes, K., and J. Broadhead. 2007. *The Role of Coastal Forests in the Mitigation of Tsunami Impacts.* F.A.O Rap Publication, Bangkok, Thailand.

Gelfenbaum G., Vatvani D., Jaffe B. and Dekker F. 2007. Tsunami Inundation and Sediment Transport in Vicinity of Coastal Mangrove Forest. *Coastal Sediments*.

Gingold, R.A., and J.J. Monaghan. 1977. Smoothed Particle Hydrodynamics: Theory and Application to Non-Spherical Stars. *Monthly Notices of the Royal Astronomical Society*: 375-389.

Harada K., Imamura F. 2005. Effect of Coastal Forest on Tsunami Hazard Mitigation - A Preliminary Investigation. *Tsunamis: Case Studies and Recent Developments*, 279-292. Springer, Netherlands.

Hiraishi T., Harada K. 2003. Greenbelt Tsunami Prevention in South-Pacific Region. *Port and Airport Research Institute*, 42: 202-213.

Hughes, S.A. 1993. "Physical Models and Laboratory Techniques in Coastal Engineering." *Advanced Series on Ocean Engineering - Volume 7*. World Scientific.

Iimura K., Tanaka N. 2012. Numerical Simulation Estimating Effects of Tree Density Distribution in Coastal Forest on Tsunami Mitigation. *Ocean Engineering,* 54: 223-232.

Irtem E., Gedik N., Kabsasli M.S. and Yasa N.E. "Coastal Forest Effects on Tsunami Run-up Heights." *Ocean Engineering*, 2009: Vol. 36, 313-320.

Liu, M.B., and G.R. Liu. 2003. *Smoothed Particle Hydrodynamics: A Meshfree Particle Method.* World Scientific Publishing, MA, USA.

Lucy, L.B. 1977. A Numerical Approach to the Testing of the Fission Hypothesis. *The Astronomical Journal*, 82: 1013-1024.

Monaghan, J.J. 1994. Simulating Free Surface Flows with SPH. *Journal of Computational Physics*, 399-405.

Monaghan, J.J. 2005. Smoothed Particle Hydrodynamics. *Reports on Progress in Physics*, 1703-1759.

Nandasena N.A.K., Tanaka N. and Tanimoto D.K. 2008. Tsunami Current Indundation of Ground with Coastal vegetation Effects: An Initial Step Towards a Natural Solution for Tsunami Amerlioration. *Journal of Earthquake Engineering and Tsunami*, 2: 157-171.

Ohira W., Honda K. and Harada K. 2012. Reduction of Tsunami Inundation by Coastal Forests in Yogyakarta, Indonesia: a Numerical Study . *Natural Hazards and Earth System Sciences*, 12: 85-95.

St-Germain P., Nistor I. and Townsend R. 2012. Numerical Modeling of the Impact with Structures of Tsunami Bores Propagating on Dry and Wet Beds using the SPH method. *International Journal of Protective Structures*, 3: 221-257.

Yanagisawa H., Koshimura S., Goto K., Miyagi T., Imamura F., Ruangrassamee A. and Tanavud C. 2009 The Reduction Effects of Mangrove Forest on a Tsunami Based on Field Surveys at Pakarang Cape, Thailand and Numerical Analysis. *Estuarine, Coastal and Shelf Science*, 81: 27-37.